Available online at www.sciencedirect.com
ScienceDirect
Journal of Hazardous Materials 157 (2008) 587–598
Journal of Hazardous Materials
www.elsevier.com/locate/jhazmat

Geopolymers for immobilization of Cr^{6+}, Cd^{2+}, and Pb^{2+}

Jianguo Zhang [a,b], John L. Provis [a,*], Dingwu Feng [a], Jannie S.J. van Deventer [a]

[a] *Department of Chemical and Biomolecular Engineering, The University of Melbourne, Victoria 3010, Australia*
[b] *Beijing Research Institute of Chemical Engineering and Metallurgy, Beijing 101149, China*

Received 18 September 2007; received in revised form 18 December 2007; accepted 10 January 2008
Available online 20 January 2008

Abstract

Alkali activation of fly ash by sodium silicate solutions, forming geopolymeric binders, provides a potential means of treating wastes containing heavy metals. Here, the effects on geopolymer structure of contamination of geopolymers by Cr(VI), Cd(II) and Pb(II) in the forms of various nitrate and chromate salts are investigated. The addition of soluble salts results in a high extent of dispersal of contaminant ions throughout the geopolymer matrix, however very little change in geopolymer structure is observed when these materials are compared to their uncontaminated counterparts. Successful immobilization of these species will rely on chemical binding either into the geopolymer gel or into other low-solubility (silicate or aluminosilicate) phases. In the case of Pb, the results of this work tentatively support a previous identification of Pb_3SiO_5 as a potential candidate phase for hosting Pb(II) within the geopolymer structure, although the data are not entirely conclusive. The addition of relatively low levels of heavy metal salts is seen to have little effect on the compressive strength of the geopolymeric material, and in some cases actually gives an increase in strength. Sparingly soluble salts may undergo some chemical conversion due to the highly alkaline conditions prevalent during geopolymerization, and in general are trapped in the geopolymer matrix by a simple physical encapsulation mechanism. Lead is in general very effectively immobilized in geopolymers, as is cadmium in all except the most acidic leaching environments. Hexavalent chromium is problematic, whether added as a highly soluble salt or in sparingly soluble form.

Keywords: Geopolymer; Aluminosilicate; Immobilization; Lead; Cadmium; Chromium

1. Introduction

With the increasing concern regarding environmental pollution and growing interest in sustainable development, the problem of heavy metal immobilization becomes even more significant. Oxidized and soluble heavy metals are significant components of many industrial and residential wastes, in particular wastes from the mining and metallurgical industries, and preventing their release into the ecosystem is of great interest. Mine tailings have long been an area of interest, and there is increasing evidence that the heavy metal contaminants present in metallurgical slags, often assumed to be effectively immobilized by ferrosilicate glasses, are in fact slightly leachable and therefore potentially problematic where slags are treated simply by dumping either in landfills or in the sea [1]. There are also numerous areas worldwide where soils have become contaminated with heavy metals over the past several decades, and the treatment of these soils to prevent further distribution of contaminants is becoming ever more critical. A number of techniques have been developed to process heavy metal-containing byproducts sufficiently and safely. Many of these approaches are based around the principle of solidification/stabilization using cement-based technologies [2,3], including alkali-activated slags and other alternative binding systems [3–5]. Geopolymeric materials have long been suggested as a material with potential value in waste treatment applications [6–10], and their use in stabilizing a variety of both toxic and radioactive wastes has been investigated over a number of years [10–15]. However, many of the exact details of the processes by which heavy metal cations are incorporated into the geopolymer structure are not yet fully understood.

Geopolymeric materials are synthesized by alkaline (hydroxide or silicate) activation of an aluminosilicate source, forming a compact gel binder phase [4]. In this investigation, fly ash from coal combustion is used as the aluminosilicate source. The chemical composition of the geopolymeric gel is generally sim-

* Corresponding author. Tel.: +61 3 8344 8755; fax: +61 3 8344 4153.
E-mail address: jprovis@unimelb.edu.au (J.L. Provis).

0304-3894/$ – see front matter © 2008 Elsevier B.V. All rights reserved.
doi:10.1016/j.jhazmat.2008.01.053

ilar to that of zeolites, but predominantly X-ray amorphous with minor crystalline inclusions [5,6]. The geopolymeric matrix provides an ideal binder for the immobilization of toxic contaminants and cationic radioactive wastes because of its low permeability, resistance to acid attack and durability in certain situations where traditional Portland cements experience problems [6,8,10,21]. In particular, resistance to chloride attack and freeze–thaw cycling degradation provide significant advantages for the use of geopolymers in immobilization applications.

Additionally, a number of the hazardous elements present in waste materials mixed with geopolymer compounds are tightly locked into the 3D network of the geopolymer bulk matrix in a strong physical or chemical way [6–9]. The mechanism of immobilization does obviously depend on the element to be immobilized [7], and geopolymers will not be universally effective in immobilizing all elements (particularly those with increased solubility under moderately alkaline conditions), but they do provide a useful component of an immobilization 'toolbox' [8].

The efficiency of heavy metal immobilization in any cement-like material is strongly related to the binder microstructure, particularly with regard to pore size distribution, pore shape, and total porosity. Deja [9] studied the immobilization of Cr^{6+}, Cd^{2+}, Zn^{2+} and Pb^{2+} in alkali-activated slag binders, and showed that microstructure and phase composition of hydrated slag play an essential role in the immobilization of heavy metals. Additionally and importantly, the metal ion itself also influences the product physical properties such as the mechanical strength. Zn^{2+} addition resulted in a decreased compressive strength whereas Cr^{6+} incorporation led to a stronger binder. van Jaarsveld and van Deventer [10] found that a small amount of Pb^{2+} increased the strength of silicate-activated fly ash/kaolinite geopolymers. However, Palomo and Palacios [11] observed a slight strength decrease in hydroxide-activated fly ash samples with a higher level of Pb^{2+} addition and a complete failure of geopolymeric setting upon addition of 2.6 wt% Cr^{6+} as CrO_3. This latter observation was attributed to the formation of $Na_2CrO_4{\cdot}4H_2O$, which then inhibited geopolymeric setting [11]. van Deventer et al. [7] also noted that immobilization of transition metals in geopolymers appears to be more problematic than when only main-group metals are involved.

It is therefore clear that much further work is required to determine the true effectiveness of geopolymers and other alkali-activated materials in waste treatment applications. Issues such as the effects of immobilized hazardous species as well as accompanying (generally non-hazardous) counterions on binder setting rates and microstructure remain in large part unknown. Given that most industrial or mining wastes contain mixtures of hazardous components, the interactions between multiple immobilized components in a single system must also be taken into consideration. For a waste treatment process to be utilizable in the real world, it must be not only effective but also economic, meaning that an inexpensive raw material such as coal fly ash is desirable. The present paper is therefore concerned with the mineralogy and microstructure of alkali-activated fly ash binders which contain heavy metal Cr^{6+}, Cd^{2+}, and Pb^{2+} ions, and the effect of these factors on metal immobilization efficiency.

2. Experimental

2.1. Materials

Coal fly ash, Class F according to ASTM C618, was obtained from Gladstone Power Station, Queensland, Australia, through Queensland Cement Limited (QCL). The fly ash has a d_{50} of 8.47 μm, with 1% of particles over 110 μm. The oxide composition as determined by X-ray fluorescence (XRF) is shown in Table 1.

Analytical-grade reagents NaOH, $Pb(NO_3)_2$, $Cd(NO_3)_2{\cdot}4H_2O$, $NaNO_3$, Na_2CrO_4, $PbCrO_4$ and Pb metal powder (−325 mesh) were obtained from Sigma–Aldrich (Australia). Medium sand (600–1180 μm) was used in preparing mortar samples. Distilled/deionized water was used throughout. Sodium silicate activating solutions ($1.5SiO_2{:}Na_2O{:}11H_2O$) were made by dissolving NaOH pellets and silica fume (Aerosil 200, Degussa) in distilled water, and were allowed to equilibrate for at least 24 h before the synthesis of geopolymers. This composition was chosen because it corresponds to the activating solution SiO_2/Na_2O ratio which gives the highest strength for geopolymers derived both from fly ash (unpublished results), and metakaolin [12,13].

2.2. Geopolymer synthesis

Fly ash, sand and heavy metal salts were dry mixed by rotating in a sealed container for 15 min. 10 M NaOH and $1.5SiO_2{:}Na_2O{:}11H_2O$ solutions were used as activators. The liquid to solid ratio (L/S) was chosen to be as low as possible while obtaining a reasonable sample rheology. For fly ash activated by $1.5SiO_2{:}Na_2O{:}11H_2O$, $L/S = 0.38$ was used. In 50% fly ash and 50% sand activated by $1.5SiO_2{:}Na_2O{:}11H_2O$, $L/S = 0.238$ gave a workable sample, and in 50% fly ash and 50% sand activated by 10 M NaOH, $L/S = 0.16$ was used. The mixed powders were combined with the solution and mixed for 30 min. Specimens were then cast in plastic molds and vibrated for 2 min to remove large air bubbles. All samples were cured at 40 °C with 100% humidity in an oven for 24 h. The samples were then demolded and sealed in plastic bags for curing at room temperature until the other tests were carried out at 7, 14 and 28 days.

Table 1
Chemical composition of fly ash as oxides

	SiO_2	Al_2O_3	Fe_2O_3	TiO_2	MnO	CaO	MgO	K_2O	Na_2O	P_2O_5	SO_3	LOI[a]
wt.%	46.4	28.3	11.7	1.4	0.2	5.1	1.4	0.6	0.3	0.9	0.3	3.3

[a] LOI: Loss on ignition at 1000 °C.

2.3. Sample analysis

Compressive strength testing was performed as per Australian Standard AS1012.9, using three 50 mm cubes of each sample composition. All samples were tested at the age of 7, 14 and 28 days. An Amsler FM 2750 (Roell Amsler, Gottmodingen, Germany) compressive strength-testing apparatus was used.

X-ray diffractometry (XRD) was conducted using a Philips PW 1800 diffractometer with Cu Kα radiation generated at 30 mA and 40 kV. Specimens were step-scanned as random powder mounts from 5 to 55° 2θ at 0.02° 2θ steps and integrated at the rate of 1.0 s per step.

Microstructural images of the fractured and carbon-coated samples were obtained using a Philips XL30 LaB_6 Scanning Electron Microscope (SEM) coupled with an Oxford Instruments EDS (ISIS ATW Si Detector) at an accelerating voltage of 20 kV.

Infrared (FTIR) spectra were collected using a Varian FTS 7000 FTIR Spectrometer in absorbance mode using a Specac MKII Golden Gate single reflectance diamond ATR attachment with KRS-5 optics. All spectra were obtained with 64 scans per spectrum.

All XRD, SEM and FTIR measurements were carried out at a sample age of 14 days. Before XRD and FTIR analysis, any added sand particles were removed from the crushed samples using a 75 μm sieve.

Static leaching tests were carried out on all samples under ambient temperature (~25 ± 5 °C) and pressure, in sealed plastic containers in order to prevent continued absorption of oxygen and carbon dioxide from the atmosphere. 32 mm × 24 mm × 22 mm cuboid samples were used, immersed in 400 ml of each leaching solution. Solutions used were:

(1) H_2SO_4, initially at pH 1.0.
(2) $MgSO_4$ at 5 wt%.
(3) Na_2CO_3 at 5 wt%.
(4) Deionized water.

The concentrations of the heavy metals in the leach solutions were measured at 21, 45, 72, 144, 240, 360, 480, 840, 1440 and 2160 h. A fresh sample was used for each time point, to avoid errors due to removal of leach solution for sampling. The concentration of each heavy metal ion in the leached solution was determined by use of an Inductively Coupled Plasma-Optical Emission Spectrometer (ICP-OES, Varian 720-ES). The pH of the H_2SO_4 and deionized water leaching solutions gradually increased throughout the experiment as alkali was leached out of the samples, and no attempt was made to maintain a constant pH in any test. Only heavy metals leaching was investigated, as the leaching of framework elements from geopolymers has been studied in some detail previously [14,15].

3. Results and discussion

3.1. Compressive strength

The compressive strengths of the geopolymers synthesized without heavy metals are presented in Table 2. From these data, it can be seen that the best mechanical compressive strength is achieved by the geopolymer paste with fly ash activated by sodium silicate. The strength of the silicate-activated mortar sample was only slightly lower after 28 days, and neither of the mortar samples showed the significant strength regression from 7 to 28 days observed in the paste sample. The significant differences in strength between pastes and mortars observed by Pacheco-Torgal et al. in geopolymers synthesized from calcined mine wastes (predominantly clays) [16] are not seen here, possibly due to the higher strength of the fly ash-based pastes here. The addition of sand also reduced the 'stickiness' of the geopolymerization slurry, making sample synthesis and handling easier, as well as reducing the *L/S* ratio which gives reduced cost and CO_2 emission [17]. Fly ash activated by 10 M NaOH does show good compressive strength, however it has previously been shown that the addition of chromium(VI) has a very detrimental effect on strength development in NaOH activation of fly ash [11]. So, the sodium silicate activator ($1.5SiO_2$:Na_2O:$11H_2O$) is chosen here for further study in immobilization of Pb, Cd and Cr. Strength data for these samples are shown in Table 3.

It must be noted that the required unconfined compressive strength for a stabilization/solidification wasteform is generally in the order of 0.7 MPa, or sometimes even lower [18]. All samples tested here are therefore seen to meet this requirement with great ease. By comparison with the compressive strengths given in Table 2 for uncontaminated samples, addition of the heavy metals has some influence on the mechanical strength of the geopolymers. Addition of lead as $Pb(NO_3)_2$ or chromium as Na_2CrO_4 actually gave an increased compressive strength at 28 days, which is a much better result compared to previous reports of a NaOH-activated fly ash with 2.60% Cr added as CrO_3, which failed to set [11]. The same authors found that 3.125% Pb as $Pb(NO_3)_2$ gave approximately 30% decrease in strength, consistent with the results of Deja [9] on sodium silicate-activated slags. The addition of Pb metal powder gave a significant improvement in strength, although the Pb powder appeared under SEM and XRD not to react to a significant extent. This may therefore be comparable to the increase in geopolymer

Table 2
The compositions and compressive strengths of geopolymer samples without heavy metals

ID	Solid components	Activator	*L/S* ratio	Compressive strength (MPa)		
				7 days	14 days	28 days
F1	50% fly ash + 50% sand	10 M NaOH	0.16	17.8	26.3	45.3
F2	Fly ash	$1.5SiO_2$:Na_2O:$11H_2O$	0.38	58.1	70.6	62.2
F3	50% fly ash + 50% sand	$1.5SiO_2$:Na_2O:$11H_2O$	0.238	41.9	62.2	60.6

Table 3
The compositions and compressive strengths of geopolymer samples with heavy metals

ID	Solid components	Activator	*L/S* ratio	Contaminant[a]	Compressive strength (MPa)		
					7 days	14 days	28 days
F4	100% fly ash	$1.5SiO_2$:Na_2O:$11H_2O$	0.38	0.5% Pb	49.5	37.0	71.2
F5	50% fly ash + 50% sand	$1.5SiO_2$:Na_2O:$11H_2O$	0.238	0.5% Pb	33.5	49.8	57.5
F6	50% fly ash + 50% sand	$1.5SiO_2$:Na_2O:$11H_2O$	0.238	0.5% Cd	38.7	51.0	61.4
F7	50% fly ash + 50% sand	$1.5SiO_2$:Na_2O:$11H_2O$	0.238	0.5% Cr	38.4	50.4	67.4
F8	50% fly ash + 50% sand	$1.5SiO_2$:Na_2O:$11H_2O$	0.238	0.5% Pb, 0.125% Cr	46.4	53.6	63.3
F9	50% fly ash + 50% sand	$1.5SiO_2$:Na_2O:$11H_2O$	0.238	1.0% Pb metal	50.9	60.2	75.5

[a] Pb and Cd added as nitrates unless otherwise noted, Cr either as sodium chromate (F7) or lead chromate (F8).

Table 4
Compressive strengths of geopolymers with and without NO_3^- (*L/S* = 0.238)

ID	Solid components	Activator	Contaminant	Compressive strength (MPa)			
				7 days	14 days	28 days	105 days
F3	50% fly ash + 50% sand	$1.5SiO_2$:Na_2O:$11H_2O$	–	41.9	62.2	60.6	70.9
F5	50% fly ash + 50% sand	$1.5SiO_2$:Na_2O:$11H_2O$	0.5% Pb as $PbNO_3$	33.5	49.8	57.5	69.5
F10	50% fly ash + 50% sand	$1.5SiO_2$:Na_2O:$11H_2O$	0.3% NO_3^- as $NaNO_3$[a]	45.7	64.5	59.2	56.6

[a] $NaNO_3$ added to give the same NO_3^- content as F5.

strength observed by Phair et al. [19] upon addition of a small percentage of (generally unreactive) ZrO_2 in powder form to a geopolymer, and attributed to nucleation effects.

Upon addition of cadmium as $Cd(NO_3)_2$, or lead and chromium as $PbCrO_4$, there is no apparent effect on the compressive strength of the geopolymeric binders. Deja [9] observed that cadmium addition as $CdCl_2$ had a significant detrimental effect on the strength of slag binders, however this may be attributed to the effects of chloride contamination of the alkali-activation process [20] rather than being specific to a cadmium salt.

On this basis, another potential complicating effect in the results presented here may be due to the NO_3^- ions introduced by addition of the heavy metals as nitrate salts. Little work has been carried out specifically to analyze the effects of nitrates in geopolymers. The nitrate ion is known to have a slight retarding effect during setting [21], and can sometimes precipitate as $NaNO_3$ [22]. Inclusion of nitrate into cancrinite-like salts has also been observed during a geopolymerization-like radioactive waste treatment process [23], however its removal by calcination is considered preferable. So, additional samples were synthesized with addition of $NaNO_3$ to give the same concentration of NO_3^- as was used in the sample with $Pb(NO_3)_2$ salt contamination (F5). A comparison of the compressive strengths of these samples and the control sample (F3) is given in Table 4.

It is interesting to note from Table 4 that the addition of $NaNO_3$ in fact gives an increased early strength (up to 14 days), but a significant regression after this, whereas $Pb(NO_3)_2$ gives a slower rate of strength development but little difference in the final strength at 105 days. It has previously been hypothesized [21] that the presence of highly soluble NO_3^- in the geopolymerization process may have some effect on the alkaline solution. The presence of a large quantity of nitrate is known to suppress silica solubility [24], although it is not clear if this is due to a simple 'salting-out' effect or an ion-specific behavior. However, at the very low levels of nitrate addition used here, any effect observed will most likely be an ion-specific one, as the effect on the ionic strength of a geopolymer pore solution of adding a small amount of $NaNO_3$ will be negligible. In any case, it is seen from Table 4 that Pb^{2+} in fact appears to be having a positive effect on the strength of the geopolymeric binder formation.

3.2. X-ray diffractometry

The XRD diffractograms of the samples with and without immobilized heavy metals are shown in Figs. 1 and 2. Fig. 1 shows diffractograms of the original fly ash as well as the uncontaminated samples, as listed in Table 2. Fig. 2 shows diffractograms of geopolymers with heavy metals as listed in Table 3.

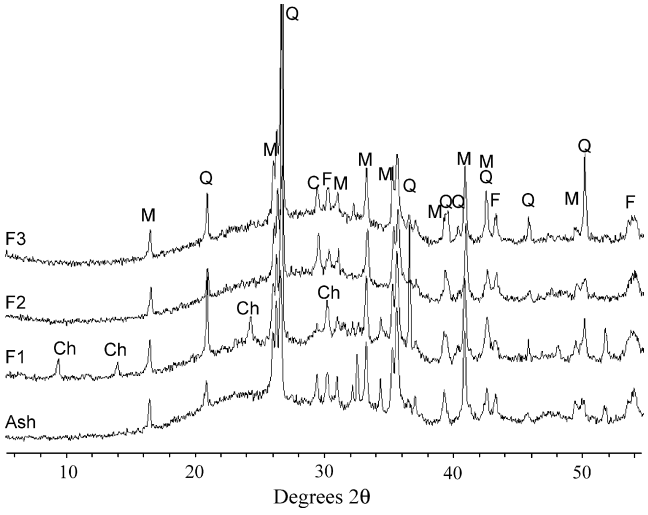

Fig. 1. The XRD diffractograms of unreacted fly ash, and uncontaminated samples (F1–F3). M: mullite; Q: quartz; C: calcite; F: Fe oxides (hematite, maghemite, magnetite); Ch: Na-chabazite.

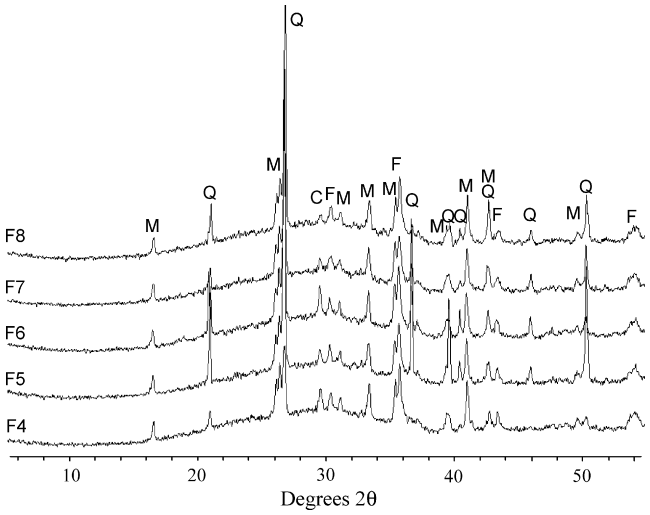

Fig. 2. The XRD diffractograms of activated fly ash containing Pb, Cd and Cr, as listed in Table 3. M: mullite; Q: quartz; C: calcite; F: Fe oxides (hematite, maghemite, magnetite).

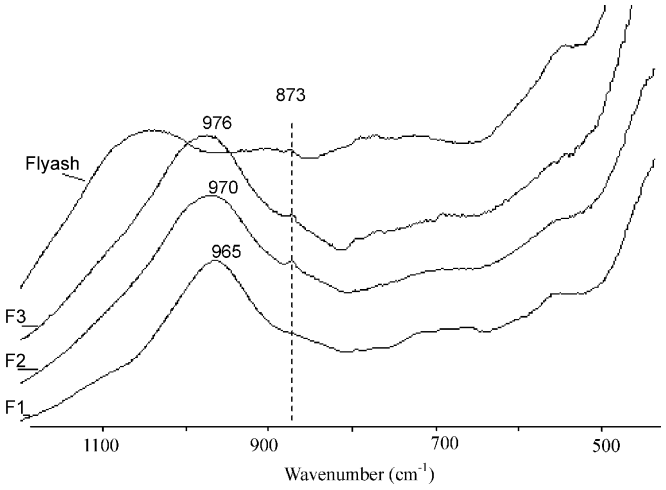

Fig. 3. FTIR spectra of the unreacted fly ash and uncontaminated geopolymer samples, as detailed in Table 2.

It is seen from Figs. 1 and 2 that quartz and mullite are observed in all the samples. These are all attributed to unreacted phases from the fly ash. Iron is present in various oxide forms in Gladstone fly ash, with hematite, magnetite and maghemite all observed [15]. These phases are not distinguished from each other in Figs. 1 and 2, as they do not appear to play a significant role in the systems studied here. This ash also contains a small quantity of calcite. A detailed investigation of the role of calcite in geopolymerization has been conducted previously [25] and will not be repeated here except to note that such a small quantity of calcite will not be expected to have a significant impact on the binder properties. This is supported by the observation that the calcite peak remains intact in all silicate-activated samples. Other small peaks due to minor crystalline ash components are not specifically assigned. The variation in the size of the quartz peaks is most likely due to different amounts of remnant quartz being left in the samples during the removal of the sand by crushing and sieving. Other than this, however, the changes observed by XRD are relatively minor. All samples show the usual 'geopolymer hump' centered at ~28–30° 2θ, and there is little notable formation of new crystalline phases.

Sample F1, activated by 10 M NaOH with *L*:*S* ratio 0.16, also contained a small quantity of zeolitic material (sodium chabazite) which was not observed in any of the silicate-activated samples but which is commonly observed in fly ash-based geopolymer synthesis. The formation of zeolites during geopolymerization has been discussed in detail elsewhere [5,26,27], with higher crystallinity observed with the use of a more highly alkaline activator, as is the case in the NaOH-activated sample here. There is also a very small peak at ~33° 2θ in each of the Pb^{2+}-contaminated samples which may correspond to the Pb_3SiO_5 phase identified by Palomo and Palacios [11,28], however this identification cannot be considered by any means conclusive. However, it does appear that the heavy metal cations are participating to some extent in the process of geopolymerization, meaning that they will be at least partially chemically bound within the geopolymer structure.

3.3. Infrared spectroscopy

Fourier transform transmission infrared spectroscopy (FTIR) is renowned for its sensitivity to structures of short-range structural order, and has been shown to be very useful in the study of geopolymers [27,29,30]. Structures of high degree order are typically characterized by sharper IR bands and greater spectral splitting than structures of low degree order. This endues FTIR as probably the most appropriate technique for studying structural evolution of amorphous aluminosilicates of high heterogeneity [20].

Figs. 3 and 4 show the FTIR spectra of unreacted fly ash, and geopolymers without and with heavy metals, respectively. The dominant Si–O–T (T = Si or Al) asymmetric stretch band is seen to move significantly to lower wavenumbers during geopolymerization with the inclusion of Al in the silicate network, consistent with detailed recent work in this area [27].

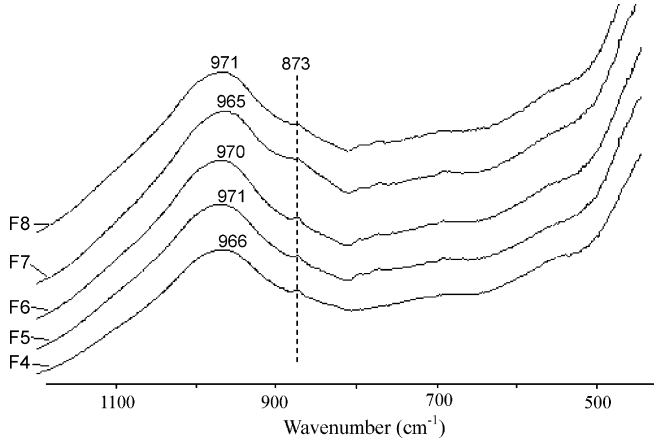

Fig. 4. FTIR spectra of the unreacted fly ash and contaminated geopolymer samples, as detailed in Table 3.

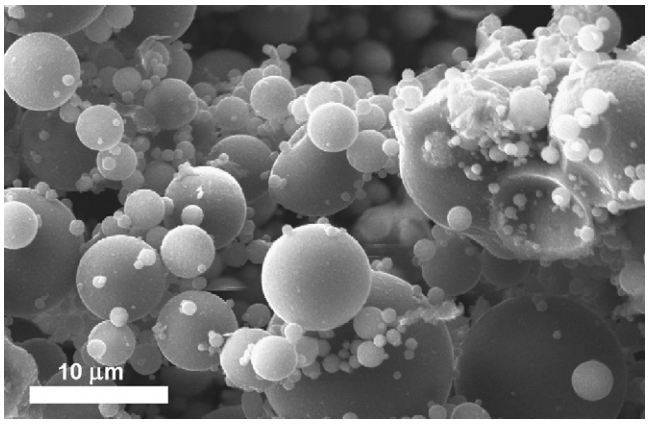

Fig. 5. SEM micrograph of the unreacted fly ash.

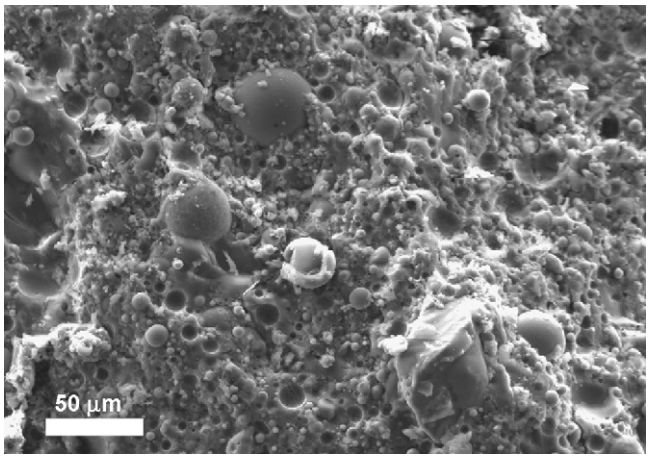

Fig. 6. SEM micrograph of a fracture surface of a geopolymer mortar (sample F3).

Rees et al. [27,31] recently showed that the relationship between Si–O–T asymmetric stretch peak position and the extent of the geopolymerization process is complex, but very instructive in the study of the mechanism of geopolymerization. However, for the purposes of this investigation, it is sufficient to note that a higher extent of Al substitution (or a higher extent of silicate depolymerization) gives a peak at lower wavenumber. Hence, F1 shows the lowest wavenumber of all uncontaminated samples. Comparing F4 to F2 shows that the addition of 0.5% Pb as $Pb(NO_3)_2$ has reduced the wavenumber of this band from 970 to 966 cm^{-1}. Similar shifts of around 4–5 cm^{-1} are observed when comparing F5, F6 and F8 to F3, with F7 (with 0.5% Cr as Na_2CrO_4) showing a shift of almost 10 cm^{-1}. The magnitudes of these shifts may be taken as being indicative of the magnitude of the effect of the contaminant ions on the geopolymer network; the strength increase upon Na_2CrO_4 addition is apparently accompanied by very significant nanostructural changes induced by the contaminant.

The bands observed at 873–874 cm^{-1} in the fly ash activated by $1.5SiO_2$:Na_2O:$11H_2O$ are associated with $CaCO_3$ vibrations [20]. The other bands observed between 500 and 800 cm^{-1} are either very broad, weak or both. However, other than the shift in the Si–O–T asymmetric stretch band as noted above, no significant differences were observed upon contamination of geopolymers with heavy metals.

3.4. Electron microscopy

SEM micrographs of the unreacted fly ash and an uncontaminated geopolymer (F3) are shown in Figs. 5 and 6. Fig. 5 gives an indication of the particle size distribution of the fly ash, which is quite broad and contains a large proportion of sub-10 μm particles. Fig. 6 shows the geopolymer matrix resulting from activation of this ash with $1.5SiO_2$:Na_2O:$11H_2O$, and indicates that the geopolymeric binder is well developed around the fly ash particles after 14 days. Trapped within the geopolymer gel (predominantly hydrated sodium aluminosilicate) is unreacted particles with a range of morphologies, corresponding to remnant phases from fly ash particles where the reactive components have dissolved. Some of these areas contain Fe-rich particles corresponding to the iron oxides observed in XRD, which appear to remain largely unreacted during geopolymerization under these conditions. Some cracking of the geopolymer samples is observed, which may be due either to mechanical damage in the sample preparation process or to drying of the samples under vacuum.

The most distinctive feature of all SEM images of fly ash-based geopolymers is that many fly ash particles are incompletely reacted, as has been discussed in some detail previously [4,32]. Fly ash is a highly heterogeneous material, which will cause interparticle variations in reactivity [32]. Different particles will also be coated to varying extents by the solidifying layer, which may also hinder the transport of dissolved components to and from the reactive surfaces [32].

Fig. 7 shows a fracture surface of sample F4, the geopolymer paste sample with 0.5% Pb as $Pb(NO_3)_2$. Fig. 7a appears to show a very similar fracture surface morphology to the uncontaminated geopolymer sample, as expected given that the contaminant levels are low. The elemental map (Fig. 7b) shows that the Pb appears to be quite well dispersed in the geopolymeric binder, although it appears to be concentrated into regions of less than a micron in size rather than being completely uniformly distributed. However, a similar analysis of the mortar sample with an identical quantity of $Pb(NO_3)_2$ (sample F5) showed that there appeared to be significant regions of Pb segregation. It may be that this is due to a higher effective contamination level in the mortar sample, where the ratio of Pb to reactive aluminosilicate components is doubled if the sand is assumed unreactive. This may therefore have been sufficient to cause phase separation of Pb-rich regions. Fig. 8 shows one such Pb-rich region in sample F5, which is >30% Pb according to EDS analysis. It is unlikely that this is undissolved lead nitrate due to the high solubility of this compound. Its Pb content may be seen to be approximately consistent with the Pb_3SiO_5 phase tentatively identified via XRD and noted previously by Palomo and Palacios [11,28]. Microscopic and XRD analysis of sample F9 (not shown), containing Pb metal powder, shows that the powder does not react to a significant extent and is essentially physically encapsulated by the geopolymer binder.

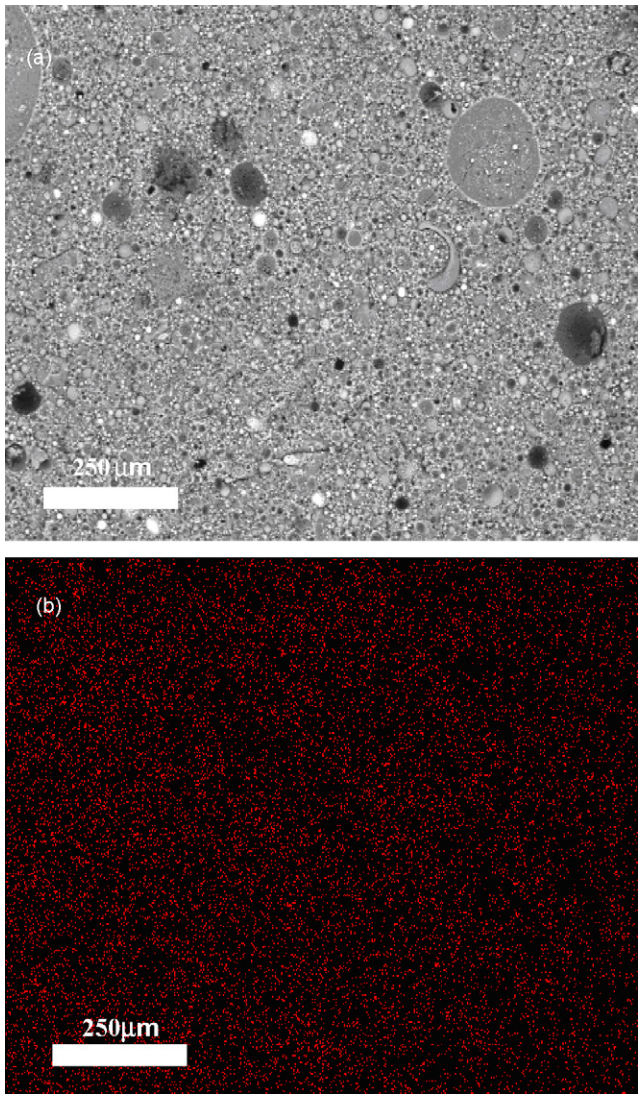

Fig. 7. SEM micrograph of fracture surface of a geopolymer paste with 0.5% Pb added as $Pb(NO_3)_2$ (sample F4): (a) backscattered electron image, and (b) Pb elemental map.

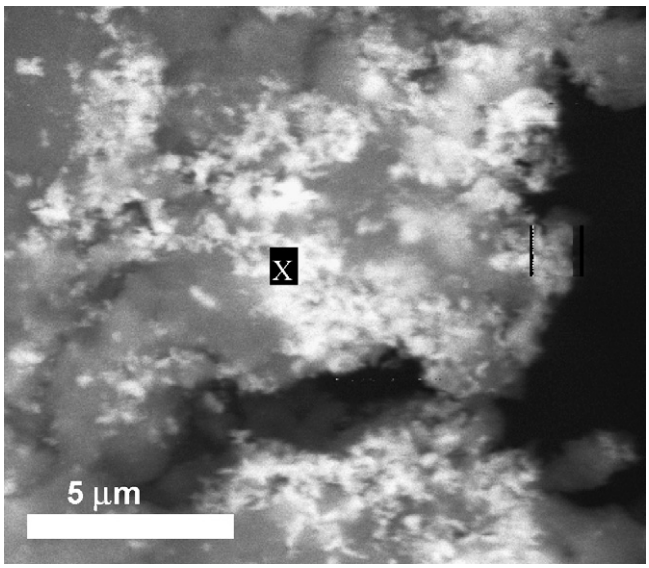

Fig. 8. SEM micrograph of fracture surface of a geopolymer mortar with 0.5% Pb added as $Pb(NO_3)_2$ (sample F5). Region marked × is >30% Pb by EDS analysis.

Fig. 9 shows an SEM micrograph of a fracture surface of sample F6, containing 0.5% Cd added as $Cd(NO_3)_2{\cdot}4H_2O$. Segregation of cadmium into specific regions of different morphology is clearly observed in this sample, with one such example shown in Fig. 9. EDS analysis shows that the elemental Cd content of this phase is around 73%. Other regions (not depicted) also show Cd contents in excess of 50% and distinct morphologies. Under the alkaline geopolymerization conditions, it appears that the $Cd(NO_3)_2{\cdot}4H_2O$ has been hydrolyzed to $Cd(OH)_2$ (76.76 element %Cd, corresponding well with the marked region in Fig. 9), as well as potentially other cadmium hydroxide and/or nitrate hydrates. $Cd(OH)_2$ formation may also be the cause of the very small XRD peak observed at ∼19° 2θ in this sample in Fig. 2, which corresponds with one of the strong peaks of one polymorph of $Cd(OH)_2$ (PDF #031-0228). The other strong peaks of this compound coincide with strong peaks of other system components in Fig. 2 and so are not available for definitive identification of this phase. However, it is likely that these hydroxide and related phases are those responsible for the immobilization of Cd^{2+} within the geopolymer matrix.

Fig. 10 shows a micrograph of the fracture surface of sample F7 (with 0.5% Cr as Na_2CrO_4), and a corresponding elemental map for Cr. The Cr appears to be very well dispersed throughout the geopolymeric binder. Addition of Cr as $PbCrO_4$ into sample F8 (not depicted) does not give the same extent of dispersion, as the sparingly soluble chromate salt particles remain to a significant extent intact throughout geopolymerization.

The results of this study in many ways follow the expected behavior of metal salts of differing solubility when exposed to an alkaline aqueous environment: the more soluble salts are well dispersed throughout the system, while the sparingly soluble salts (and Pb metal powder) either remain intact or

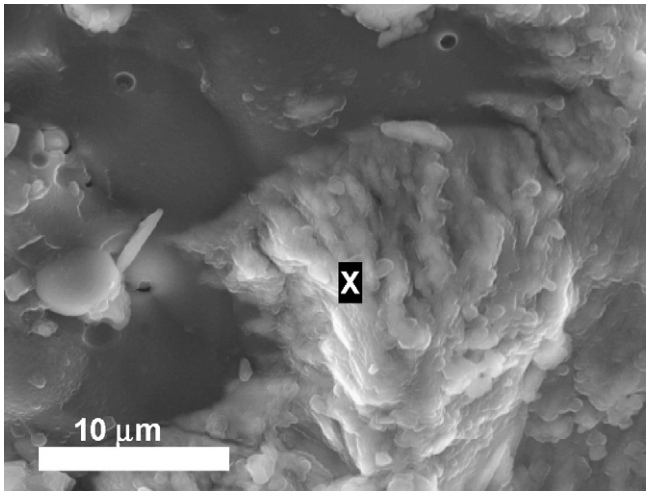

Fig. 9. SEM micrograph of fracture surface of a geopolymer mortar with 0.5% Cd added as $Cd(NO_3)_2$ (sample F6). Region marked with an × is ∼73% Cd.

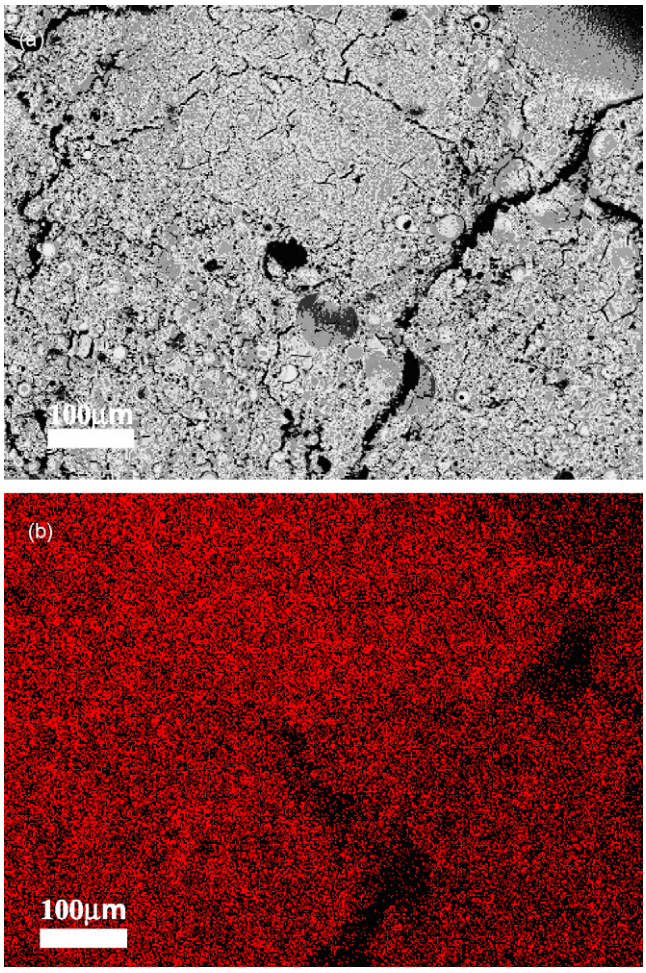

Fig. 10. SEM micrograph of fracture surface of a geopolymer with 0.5% Cr as Na_2CrO_4 (sample F7): (a) backscattered electron image, and (b) Cr elemental map.

undergo some reaction while retaining their particulate nature to a significant degree. These particles will be bound into the geopolymer matrix by relatively simple physical encapsulation, and so their leachability will be determined predominantly by the durability and permeability of the surrounding geopolymer phase. If this matrix is strong, and able to prevent leachants from contacting the encapsulated particles, then the material will be successful in immobilizing the heavy metals. Given the low solubilities of the particles, they are therefore expected to show relatively low leach rates, and could be effectively immobilized by almost any relatively durable, impermeable binder.

However, in the case of the more soluble salts such as $Pb(NO_3)_2$ or Na_2CrO_4, any significant degree of immobilization will rely on chemical binding of the contaminant elements into the geopolymer matrix structure. There may also be some extent of physical encapsulation in these samples, particularly in the case of $Pb(NO_3)_2$ where possible formation of lead silicate phases has been noted, but chemical immobilization (or its absence) will be the controlling factor in determining the leaching performance of these materials under aggressive conditions.

3.5. Leaching resistance

Here, pH 1.0 sulfuric acid solution, 5% $MgSO_4$ solution, 5% Na_2CO_3 solution and deionized water are used to leach geopolymeric matrices synthesized with the addition of Cr, Cd and Pb in different chemical forms. These leaching solutions were selected to approximate certain conditions to which geopolymers used for toxic waste immobilization may be exposed. Sulfuric acid at pH 1.0 replicates either acid mine drainage, hydrometallurgical waste or galvanizing effluent conditions. 5% $MgSO_4$ solution and 5% Na_2CO_3 solution were used to represent some of the concentrated brines or other salt solutions that may attack geopolymer structure, such as sea water, ground water, or effluents from chemical processes, mining or hydrometallurgy. Samples were immersed in the leaching solutions for periods of up to 2160 h (90 days).

Figs. 11–13 show the immobilization performance of various different geopolymer binders for treatment of Pb in various different chemical forms. These data show that, in general, Pb immobilization in geopolymers is highly effective. The highest extent of Pb leaching observed – which is seen after 90 days' immersion in H_2SO_4 – is less than 0.5%, giving an immobi-

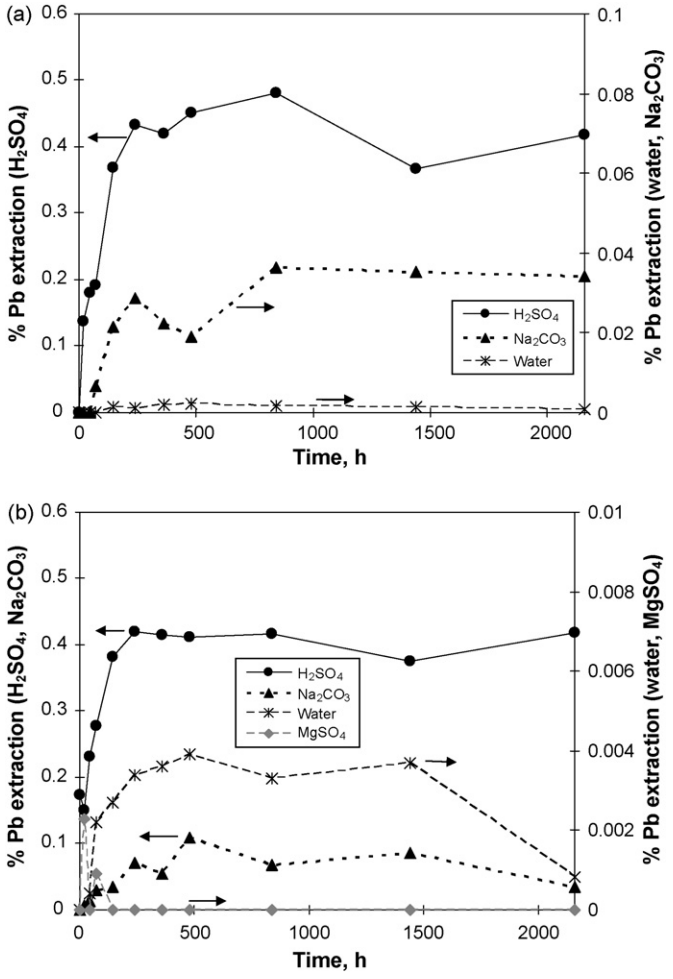

Fig. 11. Pb leaching in different aggressive solutions, from geopolymer samples with 0.5% Pb as $Pb(NO_3)_2$: (a) paste sample (F4); $MgSO_4$ leaching produced no detectable Pb release and so is not depicted, and (b) mortar sample (F5).

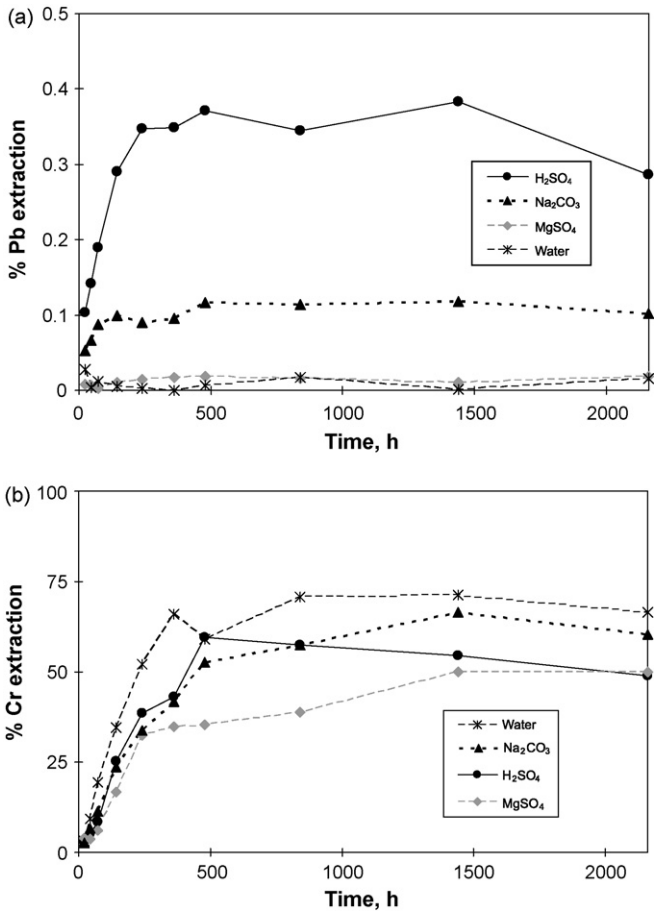

Fig. 12. Heavy metal leaching from a geopolymer mortar with 0.5% Pb and 0.125% Cr added as $PbCrO_4$ (F8), in different aggressive solutions: (a) Pb, and (b) Cr.

lization efficiency of over 99.5%. The extent of immobilization observed during leaching in deionized water is in excess of 99.9%, and the leach rates in $MgSO_4$ or Na_2CO_3 are always significantly lower than in H_2SO_4. These plots do show significant trends between samples, which provide further insight regarding

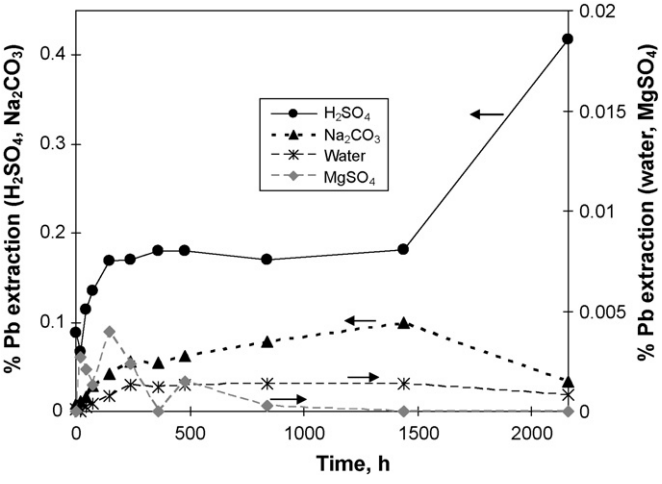

Fig. 13. Pb leaching results from a geopolymer mortar with 1% Pb metal powder (F9) in different aggressive solutions.

the exact nature of Pb immobilization in geopolymers. It is of interest that a similar degree of leaching is reached in H_2SO_4 leaching of all samples containing Pb^{2+}, which suggests that a solubility limitation (possibly $PbSO_4$) has been reached in these static batch leaching tests at ~1 ppm Pb^{2+}. Furthermore, it is observed that there appears to be some degree of reprecipitation of Pb between 60 and 90 days in many of the tests, which also suggests either some degree of solubility limitation combined with gradual formation of a lower solubility phase, or a decrease in metal solubility as the leaching pH increases with alkali release from the geopolymer pore solution.

Fig. 11 provides a comparison between sample F4, a geopolymer paste, and sample F5, a geopolymer mortar. Both samples show very low leach rates in $MgSO_4$, with Pb leaching from the paste sample being below the detection limit of ICP-OES for the entire experimental period. It is also of note that the leach rate of samples immersed in 5% Na_2CO_3 solution is significantly different from the paste to the mortar sample, with the peak Pb concentration observed in leaching of the mortar being approximately double that of the paste (note that Na_2CO_3 leaching is plotted on the right-hand vertical axis in Fig. 11a, and on the left-hand axis in Fig. 11b).

Fig. 12 shows the leach profiles of Pb and Cr from the geopolymer with these metals added as $PbCrO_4$. It was observed under SEM that the extent of dispersion of Pb and Cr through the geopolymer matrix is not high, meaning that Pb and Cr are likely to be associated with each other as $PbCrO_4$ particles encapsulated in the binder structure. However, Fig. 12 shows that the extent of Cr release during leaching is at least two orders of magnitude greater than the Pb release, regardless of the leaching environment. Comparison of Figs. 11b and 12a also shows that the release of Pb, particularly into Na_2CO_3 and $MgSO_4$ solutions, is significantly higher than when Pb was added to equivalent samples as the relatively more soluble $Pb(NO_3)_2$. These two pieces of information suggest that the Pb^{2+} is in fact being chemically bound into the geopolymer matrix wherever possible: addition as soluble $Pb(NO_3)_2$ enables this to happen early in the reaction process, whereas addition as $PbCrO_4$ means that the encapsulated $PbCrO_4$ particles must break down first. When this happens, the chromium is released into solution, while the lead is not able to migrate out of the geopolymer matrix to the same extent. Fig. 12b is the only data set in this paper showing a higher extent of leaching in water than in H_2SO_4, and the reasons for this are not clear. This cannot be due to failure of a single poorly mixed sample, as each data point in each figure represents a different replicate sample, but similar behavior is not observed in any of the other data sets shown here.

Fig. 13 shows the leaching of Pb from a geopolymer mortar containing 1% Pb as finely divided metal powder. The release of Pb in this system is generally less than when it was added in nitrate form. The H_2SO_4 leach at 90 days shows a significant spike in Pb concentration, which may be due to failure of the physical encapsulation mechanism (i.e. local microcracking leading to a lead particle becoming solubilized and dissolving in the acid solution). The $MgSO_4$ solution also appears to be showing a greater leaching extent in this system than in the others studied, or at least a delayed reprecipitation reaction. However,

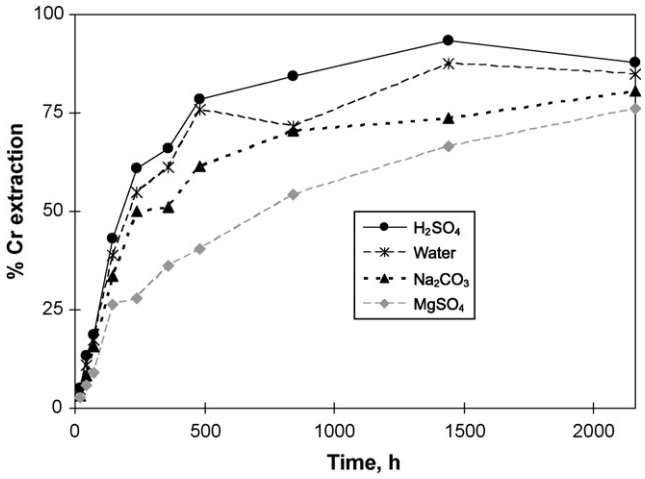

Fig. 14. Cr leaching results from a geopolymer mortar with 0.5% Cr as Na_2CrO_4 (F7) in different aggressive solutions.

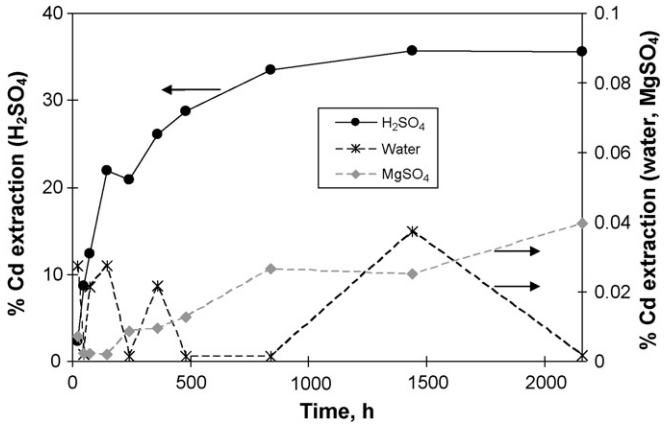

Fig. 15. Cd leaching results from a geopolymer with 0.5% Cd as $Cd(NO_3)_2$ (F6) in different aggressive solutions. Na_2CO_3 leaching solution produced no detectable leaching and so is not depicted.

the Pb concentrations in the leach solutions in all $MgSO_4$ solutions tested here are very close to the lower detection limit of the ICP-OES instrument used, due in part to the pre-analysis dilution required to avoid instrument damage by $MgSO_4$ precipitation.

It is also well known that leaching of geopolymers in acidic environments leads to release of both Si and Al from the matrix as the geopolymer structure is slightly degraded [14,15]. While similar measurements of Si and Al concentrations were not explicitly made here, the extent of heavy metal leaching will obviously correlate to at least some extent with the degree of geopolymer matrix breakdown. However, van Jaarsveld [14] showed that, in acetic acid at pH 3.3 (TCLP test conditions), both Si and Al appear to reach a solubility limitation within the first 30 h of leaching. This is much more rapid than the heavy metals extraction which is of primary interest here, showing that geopolymer matrix breakdown cannot be the sole controlling factor determining the rate of heavy metal release.

Fig. 14 shows the chromium release rate from geopolymers with 0.5% Cr as Na_2CrO_4. While the microstructural analysis and elemental mapping showed a very high extent of dispersal of the Cr throughout the geopolymer binder, the leaching data show that this formulation is actually significantly less effective in immobilizing Cr than is the mix containing $PbCrO_4$. It may be noted that the $PbCrO_4$-containing sample contained less Cr than the Na_2CrO_4-containing sample by a factor of 4. However, at the low loadings used here, and particular where the leaching is reported in terms of percentage extraction rather than as absolute concentrations, this is unlikely to be significant. The trends in Cr leaching contrast with the decreased Pb immobilization performance of the $PbCrO_4$-contaminated matrix, highlighting the importance of fully understanding the speciation and immobilization mechanisms controlling metals release. Pb is present as Pb^{2+} and is able to be chemically bound within the geopolymer, meaning that its physical encapsulation as a sparingly soluble salt is in fact less effective than being directly immobilized. On the other hand, Cr is present as CrO_4^{2-}, which is distributed throughout the geopolymer structure – most likely in pore solutions – and is not chemically bound. Its presence as a poorly soluble salt is therefore preferable, although neither example presented here shows particularly effective immobilization performance, and all leaching solutions used were rapidly turned yellow by the release of chromate. Additional and ongoing work, to be presented elsewhere [33], shows that the key to successful immobilization of Cr is control of redox chemistry within the geopolymeric binder.

Fig. 15 shows the cadmium leaching results from geopolymers with 0.5% Cd as $Cd(NO_3)_2$. It is seen that the geopolymeric binder has very good resistance to leaching by water, 5% $MgSO_4$ solution and 5% Na_2CO_3 solution. In these three leaching media, the immobilization efficiency of Cd exceeds 99.95%. However, in H_2SO_4, cadmium immobilization efficiency is low, with over 35% release in 90 days' leaching. This dramatic increase in leaching at low pH further supports the identification of a cadmium hydroxide phase as being at least partially responsible for the immobilization of Cd within the geopolymer; hydroxide salt solubility increases markedly at low pH in many cases, and this is observed here. The absence of any observable leaching into Na_2CO_3 may then be attributed to the fact that it is the most alkaline of the leach solutions used, and so has the lowest $Cd(OH)_2$ solubility. Again, it is seen that an understanding of binder chemistry is key to the effective selection of immobilization technology: leaching in deionized water, as is done in some standard leaching protocols, would show that cadmium is very effectively immobilized in geopolymers. However, if the same materials were exposed to acidic groundwater, very significant cadmium release and ensuing pollution would result.

4. Conclusions

The effect on the geopolymer structure of immobilization of heavy metal ions in geopolymeric binders depends most significantly on the form in which the contaminant is supplied. Highly soluble salts are dispersed throughout the geopolymer matrix, while sparingly soluble salts remain segregated from the bulk of the binder, although they may be converted to a dif-

ferent chemical form under the highly alkaline conditions of geopolymerization.

The predominant effect of contamination on geopolymer strength is actually seen to be caused in a number of cases by the counterions associated with heavy metals in soluble salts, in particular if nitrates are used. However, regardless of contamination levels, sodium silicate-activated fly ash geopolymers at the relatively low waste loadings tested here are able to develop strength far exceeding the requirements for a stabilization/solidification wasteform. Earlier negative results (lack of strength development) in the treatment of Cr(VI) by NaOH activation of fly ash are not repeated in the case of silicate activation. Some heavy metal contaminated wasteforms actually developed a strength exceeding that of their uncontaminated counterparts.

The resistance of heavy-metal-containing geopolymers to leaching in different environments depends very strongly on both the nature of the heavy metal and the aggressive components of the leaching solution. H_2SO_4 leaching in general shows a higher rate of metals release than the other leach solutions tested. Pb is immobilized very effectively by a chemical binding mechanism in geopolymers, meaning that its addition in a soluble chemical form is actually preferable. Cr(VI) immobilization is quite ineffective, although its addition as a sparingly soluble salt is somewhat better than as a soluble salt. Cd immobilization depends on the solubility of a hydroxide phase, and so is very effective at high pH but poor at low pH. This work further reinforces the need for a scientific basis underpinning the choice of any binder for waste immobilization, with almost all variations in leaching performance between systems able to be explained by analysis of the binder chemistry.

Acknowledgements

The authors thank the Particulate Processing Centre (a Special Research Centre of the Australian Research Council), and The China Scholarship Council, for financial support of this research.

References

[1] A. Kontopoulos, K. Komnitsas, A. Xenidis, Environmental characterisation of the lead smelter slags in Lavrion, in: Proceedings of the IMM Minerals Metals and the Environment II Conference, Prague, 1996.
[2] F.P. Glasser, Fundamental aspects of cement solidification and stabilisation, J. Hazard. Mater. 52 (2–3) (1997) 151–170.
[3] R. Malviya, R. Chaudhary, Factors affecting hazardous waste solidification/stabilization: a review, J. Hazard. Mater. B137 (2006) 267–276.
[4] P. Duxson, A. Fernández-Jiménez, J.L. Provis, G.C. Lukey, A. Palomo, J.S.J. van Deventer, Geopolymer technology: the current state of the art, J. Mater. Sci. 42 (9) (2007) 2917–2933.
[5] J.L. Provis, G.C. Lukey, J.S.J. van Deventer, Do geopolymers actually contain nanocrystalline zeolites?—a reexamination of existing results, Chem. Mater. 17 (12) (2005) 3075–3085.
[6] C. Shi, P.V. Krivenko, D.M. Roy, Alkali-Activated Cements and Concretes, Taylor & Francis, Abingdon, UK, 2006, 376 pp.
[7] J.S.J. van Deventer, J.L. Provis, P. Duxson, G.C. Lukey, Reaction mechanisms in the geopolymeric conversion of inorganic waste to useful products, J. Hazard. Mater. A139 (3) (2007) 506–513.
[8] N.B. Milestone, Reactions in cement encapsulated nuclear wastes: need for toolbox of different cement types, Adv. Appl. Ceram. 105 (1) (2006) 13–20.
[9] J. Deja, Immobilization of Cr^{6+}, Cd^{2+}, Zn^{2+} and Pb^{2+} in alkali-activated slag binders, Cement Concrete Res. 32 (12) (2002) 1971–1979.
[10] J.G.S. van Jaarsveld, J.S.J. van Deventer, The effect of metal contaminants on the formation and properties of waste-based geopolymers, Cement Concrete Res. 29 (8) (1999) 1189–1200.
[11] A. Palomo, M. Palacios, Alkali-activated cementitious materials: Alternative matrices for the immobilisation of hazardous wastes—Part II. Stabilisation of chromium and lead, Cement Concrete Res. 33 (2) (2003) 289–295.
[12] P. Duxson, J.L. Provis, G.C. Lukey, S.W. Mallicoat, W.M. Kriven, J.S.J. van Deventer, Understanding the relationship between geopolymer composition, microstructure and mechanical properties, Colloids Surf. A—Physicochem. Eng. Asp. 269 (1–3) (2005) 47–58.
[13] P. Duxson, S.W. Mallicoat, G.C. Lukey, W.M. Kriven, J.S.J. van Deventer, The effect of alkali and Si/Al ratio on the development of mechanical properties of metakaolin-based geopolymers, Colloids Surf. A—Physicochem. Eng. Asp. 292 (1) (2007) 8–20.
[14] J.G.S. van Jaarsveld, Ph.D. Thesis, University of Melbourne, Australia, 2000, 381 pp.
[15] R.R. Lloyd, Ph.D. Thesis, University of Melbourne, Australia, to be submitted.
[16] F. Pacheco-Torgal, J. Castro-Gomes, S. Jalali, Investigations about the effect of aggregates on strength and microstructure of geopolymeric mine waste mud binders, Cement Concrete Res. 37 (6) (2007) 933–941.
[17] P. Duxson, J.L. Provis, G.C. Lukey, J.S.J. van Deventer, The role of inorganic polymer technology in the development of 'Green concrete', Cement Concrete Res. 37 (12) (2007) 1590–1597.
[18] C.D. Hills, S.J.T. Pollard, The influence of interference effects on the mechanical, microstructural and fixation characteristics of cement-solidified hazardous waste forms, J. Hazard. Mater. 52 (2–3) (1997) 171–191.
[19] J.W. Phair, J.S.J. van Deventer, J.D. Smith, Mechanism of polysialation in the incorporation of zirconia into fly ash-based geopolymers, Ind. Eng. Chem. Res. 39 (8) (2000) 2925–2934.
[20] W.K.W. Lee, J.S.J. van Deventer, The effects of inorganic salt contamination on the strength and durability of geopolymers, Colloids Surf. A—Physicochem. Eng. Asp. 211 (2–3) (2002) 115–126.
[21] W.K.W. Lee, J.S.J. van Deventer, The effect of ionic contaminants on the early-age properties of alkali-activated fly ash-based cements, Cement Concrete Res. 32 (4) (2002) 577–584.
[22] M.G. Blackford, J.V. Hanna, K.J. Pike, E.R. Vance, D.S. Perera, Transmission electron microscopy and nuclear magnetic resonance studies of geopolymers for radioactive waste immobilization, J. Am. Ceram. Soc. 90 (4) (2007) 1193–1199.
[23] Y. Bao, M.W. Grutzeck, C.M. Jantzen, Preparation and properties of hydroceramic waste forms made with simulated Hanford low-activity waste, J. Am. Ceram. Soc. 88 (12) (2005) 3287–3302.
[24] C.F. Weber, R.D. Hunt, Modeling alkaline silicate solutions at 25 °C, Ind. Eng. Chem. Res. 42 (26) (2003) 6970–6976.
[25] C.K. Yip, Ph.D. Thesis, University of Melbourne, Australia, 2004, 389 pp.
[26] M. Criado, A. Fernández-Jiménez, A.G. de la Torre, M.A.G. Aranda, A. Palomo, An XRD study of the effect of the SiO_2/Na_2O ratio on the alkali activation of fly ash, Cement Concrete Res. 37 (5) (2007) 671–679.
[27] C.A. Rees, J.L. Provis, G.C. Lukey, J.S.J. van Deventer, ATR-FTIR analysis of fly ash geopolymer gel ageing, Langmuir 23 (15) (2007) 8170–8179.
[28] M. Palacios, A. Palomo, Alkali-activated fly ash matrices for lead immobilisation: a comparison of different leaching tests, Adv. Cement Res. 16 (4) (2004) 137–144.
[29] W.K.W. Lee, J.S.J. van Deventer, The use of infrared spectroscopy to study geopolymerization of heterogeneous amorphous aluminosilicates, Langmuir 19 (21) (2003) 8726–8734.
[30] M. Criado, A. Fernández-Jiménez, A. Palomo, Alkali activation of fly ash. Effect of the SiO_2/Na_2O ratio. Part I: FTIR study, Microporous Mesoporous Mater. 106 (1–3) (2007) 180–191.

[31] C.A. Rees, J.L. Provis, G.C. Lukey, J.S.J. van Deventer, In situ ATR-FTIR study of the early stages of fly ash geopolymer gel formation, Langmuir 23 (17) (2007) 9076–9082.

[32] A.M. Fernández-Jiménez, E.E. Lachowski, A. Palomo, D.E. Macphee, Microstructural characterisation of alkali-activated PFA matrices for waste immobilisation, Cement Concrete Compos. 26 (8) (2004) 1001–1006.

[33] J. Zhang, J.L. Provis, D. Feng, J.S.J. van Deventer, The role of sulfide in the immobilization of Cr(VI) in fly ash geopolymers, Cement Concrete Res., 2008, in press.